Molecular Dynamics Simulation on Corrosion Interface of α-Iron and Liquid Lead: Benchmark Test of Machine Learning Potential

Seoyeon Bak, Takuji Oda*
Dept. of Energy Systems Engineering, Seoul Natl. Univ., 1 Gwanak-ro, Gwanak-gu, Seoul 08826
**Corresponding author: oda@snu.ac.kr*

1. Introduction

Liquid lead (Pb) or lead-bismuth eutectic (LBE) has promising properties to be applied in fast reactor design such as low neutron absorption, wide liquid temperature range and high thermal conductivity. A pending engineering issue in the lead-cooled fast reactors (LFRs) including the accelerator driven subcritical reactor (ADSR) is corrosion of structural materials. Iron (Fe) based steels such as ferritic/martensitic (F/M) steel and austenitic stainless steel (AuSS) have been considered as the structural materials. Steel corrosion is especially severe at high temperatures as the solubility of the steel component increases with temperature. Furthermore, above 800 K, the oxide film acting as the passivation layer was observed to be permeable [1]. For example, in T91 steel, 1250 hours of exposure to LBE resulted in corrosion of Fe matrix even though the impaired oxide film remained [2].

For better corrosion control, understanding intermetallic corrosion mechanisms is important; however, it is yet to be achieved even between the most basic elements. Moreover, the quantitative data on relevant properties such as solubility still need to be refined. Density functional theory (DFT) is an elaborate electronic structure approach in the field of computational materials science and engineering and is potentially applicable to materials corrosion studies. However, its high computational cost makes large-scale and long-time simulations difficult, and thus the applicability to complex systems and phenomena is limited.

Recently, machine learning (ML) potential has been emerging as an alternative to imitate the DFT while benefiting feasible speed of molecular dynamics (MD). Quaranta et al. captured the structure and dynamics of the interface of liquid water and zinc-oxide employing a neural network potential (NNP) with near DFT accuracy at a fraction of the cost [3].

In this study, a moment tensor potential (MTP) is developed as it is well balanced in both accuracy and computational efficiency [4]. Herein, the performance of the MTP is validated, and the corrosion phenomenon observed in the MD simulation is discussed preliminarily.

2. Methods

In this section, the methodology to construct the MTP using the Machine Learning Interatomic Potential (MLIP) package [4] is described.

2.1 Construction of Moment Tensor Potential

The potential energy of an atom is expressed as a linear combination of a set of basis functions represented to be the descriptor to capture the local atomic environment, and the coefficients are the fitting parameters. The basis functions are comprised of radial and angular parts. The radial part is composed of polynomials operant within $[R_{min}, R_{max}]$ while the angular part is composed of moment tensors. The so-called level of moments is introduced as a measure of the size of basis. MTP includes all basis functions whose level is less than or equal to the specified maximum level lev_{max}.

Let the training data of total K configurations contain the DFT data of energy $E^{dft}(cfg_k)$, force for ith atom $f_i^{dft}(cfg_k)$ and stress $\sigma^{dft}(cfg_k)$ for k th configuration cfg_k. Then, the parameters θ, which is composed of coefficients of radial and angular basis functions, are searched to minimize the loss function as follows

$$\sum_{k=1}^{K}\Big[w_e\left(E^{mtp}(cfg_k;\theta)-E^{dft}(cfg_k)\right)^2+ w_f\sum_{i=1}^{N_k}\left|f_i^{mtp}(cfg_k;\theta)-f_i^{dft}(cfg_k)\right|^2+ w_s\left|\sigma^{mtp}(cfg_k;\theta)-\sigma^{dft}(cfg_k)\right|^2\Big]\rightarrow \min_{\theta} \quad (1)$$

where N_k is the number of atoms in the k th configuration, and w_e, w_f and w_s are the weights for energy, force and stress, respectively. To balance the computational burden and the accuracy, we performed test calculations changing hyperparameters such as R_{min}, R_{max} and lev_{max}. It was confirmed the training root mean square error (RMSE) in energy fitting converges to about 6 meV/atom if R_{min}, R_{max} and lev_{max} are 1.5 Å, 6.0 Å and 16, respectively.

2.2 Generation of Training Data

All the training data were generated from first principles (FP) calculations based on DFT using the Vienna Ab initio Simulation Package (VASP) [5]. To estimate the exchange-correlation (XC) energy, the regularized-restored strongly constrained and appropriately normed (r^{2}SCAN) functional [6] was employed as it is in balance to describe both of Fe and Pb. The effect of core electrons was described by the projector augmented wave (PAW) method, and the valence electrons were represented by a plane-wave basis with an energy cutoff of 470 eV. The band energy

was calculated using the first order Methfessel-Paxton method [7] of a 0.2 eV smearing width over a Monkhorst-Pack grid [8] with a spacing of 0.025 $Å^{-1}$.

MTP was constructed by combining supervised and active learning. First, for the supervised learning, the initial training data were collected from static calculation, geometry optimization and FP-MD on bulk, surface and interface systems at sparse temperatures of 500 K, 1000 K and 2000 K. The configurations bring together a variety of phases, densities and shapes, and some of which contain point defects such as vacancy, interstitial and substitutional. The surface and interface were modeled on the basis of three low index surfaces of bcc-Fe (i.e., (100)/(110)/(111)). Afterward, the training data corresponding to (100) bcc-Fe and liquid Pb interface were efficiently expanded under the active learning scheme.

The active learning implemented in the MLIP package uses a query strategy in which the MTP itself picks out additional training data to learn on-the-fly during MD simulations [4]. The so-called extrapolation grade which is a measure of the novelty of a given configuration compared to the ones already in the training data is evaluated for every configuration. It postulates that a good training data corresponds to the one with which the determinant of the linear system to be solved is maximum. Then, only the configurations of which extrapolation grades satisfy the specified criteria are the candidates to be the training data. Among those extrapolative configurations, non-repetitive and representative configurations are finally selected. The selected configurations are processed by the DFT and appended to the training data. This scheme was repeated until any local atomic environments that appeared during the interface simulation were interpolated or mildly extrapolated from the training data of MTP.

2.3 Correction via Two-Body Potential

The accuracy of DFT calculation depends on the XC functional used. For mixtures, it is desirable to choose a one that can achieve sufficient accuracy for all compounds and states that may occur. After comparing several functionals, the r^{2}SCAN functional was selected because it performed the best. However, it overestimated the absolute value of cohesive energy of Fe corresponding to the energy of the reference state, namely α phase, relative to that of isolated gas. As dissolution is a process wherein Fe escapes from the reference state, this energy level needs to be accurately produced. To correct this systematic weakness, a slight two-body (2B) potential was added for Fe-Fe interatomic potential energy in the following form

$$f_{2B}(|r_{ij}|) = \begin{cases} C_1(C_2 - |r_{ij}|)^3 |r_{ij}|^{C_3} & |r_{ij}| < R_{max} \\ 0 & |r_{ij}| \geq R_{max} \end{cases} \quad (2)$$

where r_{ij} is the position of the neighboring jth atom relative to the ith atom, and C_1, C_2 and C_3 were set to 0.00056, 6 and 0.5, respectively. These values were optimized to reproduce the experimental cohesive energy of Fe.

3. Results and Discussions

Hereafter, all the static or MD simulations with the MTP were performed using the Large-scale Atomic Molecular Massively Parallel Simulator (LAMMPS) [9] which provides an interface with the MLIP package [4].

3.1 Cohesive Properties of Fe and Pb

The cohesive properties of bcc-Fe and fcc-Pb calculated with the MTP are summarized and compared with experiment in Table 1 [10,11]. It is shown in Table 1 that the MTP successfully reproduces the experimental cohesive energy of Fe owing to the 2B correction. In the case of Pb, there is an undeniable discrepancy with experiment. Nevertheless, we consider it acceptable as Pb does not form a solid phase in the conditions assumed in the present study.

Table 1. Lattice constant (in Å) and cohesive energy (in eV) calculated at 0 K for bcc-Fe and fcc-Pb using the MTP in comparison with experiment [10,11].

		a_0 [10]	E_0 [11]
Fe	MTP	2.895	-4.28
	Exp.	2.858	-4.28
Pb	MTP	4.984	-2.86
	Exp.	4.920	-2.03

3.2. Solution Enthalpy of Fe in Liquid Pb

Since the corrosion results in the formation of solute Fe in liquid Pb, the solution enthalpy is an important quantity to be assessed. The solution enthalpy of Fe in liquid Pb is defined as the amount of the enthalpy needed for a Fe atom to dissolve in liquid Pb escaping from the reference state at a given temperature as

$$\Delta H_{sol} = H[m\ Pb\ (l) + Fe\ (solute)] - m\ H[Pb\ (l)] - H[Fe\ (s)] \quad (3)$$

where $H[m\ Pb\ (l) + Fe\ (solute)]$, $H[Pb\ (l)]$ and $H[Fe\ (s)]$ are the enthalpy of liquid Pb containing a solute Fe atom (Pb_mFe_1), per-atom enthalpy of liquid Pb and per-atom enthalpy of solid bcc-Fe, respectively. The experimental solution enthalpy can be derived from the experimental solubility as the slope in the Arrhenius plot, and thus assumed to be a constant independent of temperature. The solution enthalpy of Fe in liquid Pb was calculated from MD simulation with the MTP in an NPT ensemble for each system. The calculated results at intervals of 100 K from 700 K to 1400 K are plotted in Fig. 1 in comparison with the recommended value from thermodynamic assessment of some experimental data

[12]. Although the calculation results were in reasonable agreement with the recommended value, the calculations suggested that the solution enthalpy is temperature dependent.

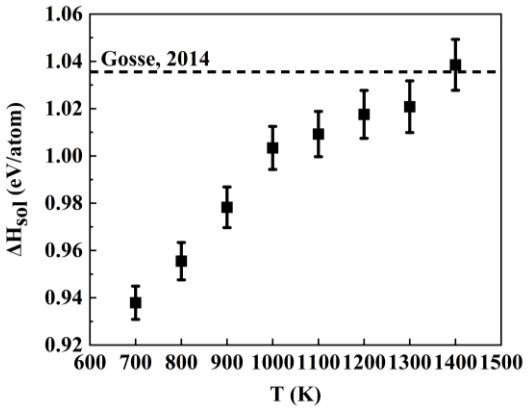

Figure 1. Solution enthalpy of bcc-Fe in liquid Pb calculated at intervals of 100 K from 700 K to 1400 K using the MTP in comparison with the recommended value from thermodynamic assessment of experimental data [12].

3.3. Molecular Dynamics Simulation on Fe-Pb Interface

Finally, the corrosion phenomenon at the (100) bcc-Fe and liquid Pb interface was simulated by MD with the MTP in an NPT ensemble. Fig. 2 shows snapshots of MD simulations performed at 800 K and 1200 K with structure analysis. If we consider the interface as the layer where the bcc structure is destroyed, the thickness of the interface seemed to increase with temperature. It is intuitive that the more corroded bcc-Fe is, the weaker the bonding stability and the more disordered the structure becomes at the surface.

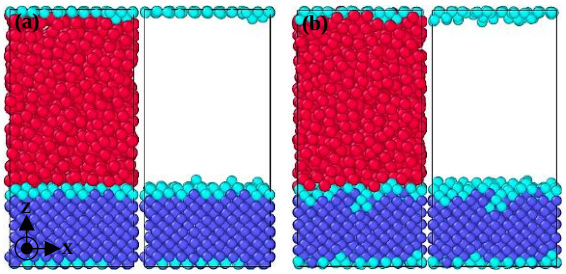

Figure 2. Snapshots of MD simulation with the MTP on (100) bcc-Fe and liquid Pb interface in an NPT ensemble (a) at 800 K and (b) at 1200 K with structure analysis. The accompanying figures are versions with Pb hidden to clearly show the interface. Blue, cyan and red spheres denote bcc-Fe, disordered Fe and Pb, respectively.

To quantitatively estimate the corrosion behavior, the concentration of Fe dissolved in liquid Pb was obtained as a function of time by simulating the interface composed of 162,000 Fe atoms and 120,000 Pb atoms at 1100 K. The result is shown in Fig. 3. Fe in contact with liquid Pb corroded and thus dissolved, although in small amounts. Thermodynamically, the concentration converges to a certain value, corresponding to the solubility at equilibrium. In Fig. 3, the concentration still fluctuates within a range because some of the dissolved Fe deposited on the surface of bcc-Fe. We plan to determine the corrosion rate and equilibrium solubility by conducting long simulations of multiples samples to improve statistical precision in a future study.

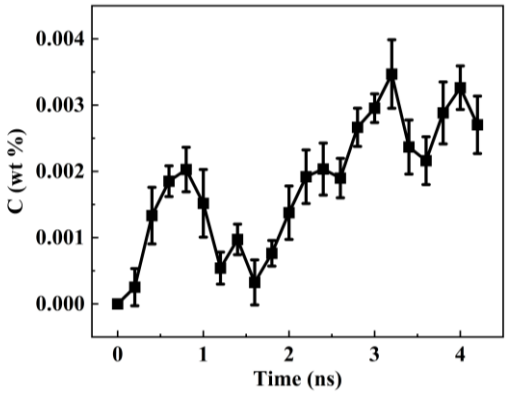

Figure 3. Concentration of Fe dissolved in liquid Pb as a function of time from MD simulation with the MTP on (100) bcc-Fe and liquid Pb interface in an NPT ensemble at 1100 K.

4. Conclusions

As a first step to understand the microscopic corrosion mechanisms, an accurate and fast MTP was developed to simulate the corrosion interface of α-Fe and liquid Pb. The MTP reasonably reproduced the cohesive properties of Fe and Pb. The solution enthalpy of Fe in liquid Pb, which is a key quantity related to corrosion, was calculated from MD simulation with the MTP at a wide temperature range and was in reasonable agreement with the recommended experimental value. The MD simulation was performed with the MTP on the (100) bcc-Fe and liquid Pb interface at varying temperatures, visualizing the corroding interface. The corrosion damage was preliminarily analyzed through the time evolution of the concentration of Fe dissolved in liquid Pb.

Given the overall performance and the interface simulation results, we expect that the present MTP can be used in the future to predict corrosion related properties such as corrosion rate and solubility and to study mitigation strategies.

ACKNOWLEDGEMENTS

This research was supported by the National Research Foundation (NRF) of Korea grant funded by the Korean government (MSIT) (No. 2021R1F1A1063748), and the Brain Korea 21 FOUR Program (No. 4199990314119).

REFERENCES

[1] F. J. Martín, L. Soler, F. Hernández and D. Gómez-Briceño, “Oxide layer stability in lead-bismuth at high temperature.” J. Nucl. Mater., 335.2, 194–198, (2004).

[2] D. Sapundjiev, S. Van Dyck and W. Bogaerts, “Liquid metal corrosion of T91 and A316L materials in Pb-Bi eutectic at temperatures 400-600 °C.” Corros. Sci., 48.3, 577–594, (2006).
[3] V. Quaranta, J. Behler and M. Hellström, “Structure and dynamics of the liquid–water/zinc-oxide interface from machine learning potential simulations.” J. Phys. Chem. C, 123.2, 1293–1304, (2019).
[4] I. S. Novikov, K. Gubaev, E. V. Podryabinkin and A. V. Shapeev, “The MLIP package: moment tensor potentials with MPI and active learning.” Mach. Learn. Sci. Technol., 2.2, 025002, (2020).
[5] G. Kresse and J. Furthmü, “Efficient iterative schemes for ab initio total-energy calculations using a plane-wave basis set.” Phys. Rev. B, 54.16, 11169, (1996).
[6] J. W. Furness, A. D. Kaplan, J. Ning, J. P. Perdew and J. Sun, “Accurate and numerically efficient r2SCAN meta-generalized gradient approximation.” J. Phys. Chem. Lett., 11.19, 8208–8215, (2020).
[7] M. Methfessel and A. T. Paxton, “High-precision sampling for Brillouin-zone integration in metals.” Phys. Rev. B, 40.6, 3616, (1989).
[8] H. J. Monkhorst and J. D. Pack, “Special points for Brillouin-zone integrations.” Phys. Rev. B, 13.12, 5188, (1976).
[9] S. Plimpton, “Fast parallel algorithms for short-range molecular dynamics,” J. Comput. Phys, 117.1, 1–19, (1993).
[10] Davey and P. Wheeler, “Precision measurements of the lattice constants of twelve common metals.” Phys. Rev., 25.6, 753, (1925).
[11] C. Kittel and P. McEuen, "Introduction to solid state physics. Vol. 8.” Wiley, (1996).
[12] S. Gossé, “Thermodynamic assessment of solubility and activity of iron, chromium, and nickel in lead bismuth eutectic.” J. Nucl. Mater. 449.1–3, 122–131, (2014).